The switch from bacterial phosphorus mineralization to arbuscular mycorrhiza in root hairless wheat during crop development

Courtney Horn Herms[1], Ian Tsang[2,3], Frederik Bak[1], Klara Gunnarsen[1], Magdalena Hasenzagl[1], Amaru Miranda Djurhuus[1], Tom Thirkell[4], Eric Ober[2], Fiona Leigh[2], James Cockram[2], Mette Haubjerg Nicolaisen[1]

1) Department of Plant and Environmental Sciences, University of Copenhagen, Thorvaldsensvej 40, 1871 Frederiksberg, Denmark

2) Niab, Park Farm, Histon, Cambridge, CB24 9NZ, United Kingdom

3) School of Biosciences, University of Nottingham, Sutton Bonington, Loughborough LE12 5RD, United Kingdom

4) Department of Plant Sciences, University of Cambridge, Cambridge, CB3 0LE, United Kingdom

Corresponding Author: Mette Haubjerg Nicolaisen; email: meni@plen.ku.dk

ORCIDs: C.H.H.: 0000-0002-7363-3189; I.T.: 0009-0006-1999-3251; F.B.: 0000-0001-9580-8018; K.G.: 0000-0001-8176-8844; M.H.: no ORCID; A.M.D.: 0000-0003-3762-2922; T.T.: 0000-0002-4481-0924; E.O.: 0000-0002-4832-5897; F.L.: 0000-0002-3221-5327; J.C.: 0000-0002-1014-6463; M.H.N.: 0000-0002-0983-2466

Abstract

Understanding how crops recruit bacterial and fungal partners for phosphorus (P) nutrition remains incomplete, particularly regarding temporal shifts between P-cycling bacteria and arbuscular mycorrhizal fungi (AMF). We investigated these dynamics using the wheat root hair mutant *short root hair* 1 (srh1), which is impaired in root hair elongation and may be more dependent on microbial P acquisition compared to the wildtype. We profiled the P-cycling bacterial microbiome and AMF colonization across development and at booting under P-depleted conditions. Before AMF establishment, the root hair mutant rhizosphere was enriched in bacterial organic P-mineralization genes. After AMF colonization increased in both genotypes, this enrichment disappeared, indicating a temporal shift from bacterial to fungal P acquisition. Growing the root hair mutant in P-depleted conditions to booting, when P uptake is highest in wheat, did not induce the mutant to recruit its bacterial P-cycling microbiome. Instead, AMF arbuscule formation was enriched. Collectively, our results reveal a temporal

transition in wheat from bacterial to AMF-mediated P nutrition and highlight the compensatory role of the microbiome in plants lacking root hair elongation.

Key Words

Arbuscular mycorrhizha, phosphorous-solubilizing microorganisms, plant-microbe interactions, root microbiome, root hairs, plant phosphorus nutrition, *Triticum aestivum* (wheat)

Introduction

Agricultural productivity is often constrained by nutrient availability. Phosphorus (P) is an essential nutrient and vital for central biochemical processes in the plant (Rengel et al., 2022). Despite relatively large amounts of total P in most agricultural soils, bioavailability of P is limited, leading to restricted plant growth and yield (Menezes-Blackburn et al., 2018). Thus, P is one of the most heavily applied nutrients to agricultural fields. P fertilizer is, however, poorly absorbed by the plant (Simpson et al., 2011), leading to risks of environmental runoff and eutrophication (Ulén et al., 2007). Furthermore, raw phosphate rock used to make P fertilizer is a finite resource with high energy demands for production (Van Kauwenbergh, 2010), further impacting the sustainability of current P fertilization practices. The need to grow more food using reduced P inputs requires the development of new methods to improve crop P nutrition under reduced chemical fertilizer amendments.

The plant utilizes several methods to ensure P nutrition. Root hairs help the plant access greater volumes of soil and improve P uptake (Bates & Lynch, 1996; Gahoonia et al., 2001). In addition, the plant root microbiome plays an important role in plant P nutrition. The fungal fraction of the microbiome, notably the arbuscular mycorrhizal fungi (AMF), play a vital role in accessing soil P and providing mineral P to their host plant, including in globally important crops such as wheat (*Triticum aestivum* L.) (Thirkell et al., 2020). In low-P conditions, AMF colonization is enriched to improve crop P uptake (Breuillin et al., 2010). Similarly, in root hairless crops, AMF take over the role of root hairs in P uptake in accordance with the root economics spectrum (Kumar et al., 2019; Wang et al., 2025). AMF colonize plant roots at a defined point in root development; in field-grown wheat, this correlates to growth stage (GS) 12 (Marrassini et al., 2024) on Zadok's scale of wheat development (Zadoks et al., 1974), where two leaves are fully unfolded.

The bacterial fraction of the plant root microbiome is initially recruited from the seed-borne microbial community (Simonin et al., 2022). From the seed and throughout germination and development, the plant develops its bacterial microbiome to assist in P cycling (Xiong et al., 2021; Nunes et al., 2022) and to alleviate P stress when P uptake is limited (Tang et al., 2022; Zhang et al., 2025). Organic P mineralization is represented by bacterial genes such as *bpp* (beta propeller phytase), *phnK* (phosphonate degradation), *phoD* (cytoplasmic phosphatase), and *phoX* (periplasmic phosphatase). Bacterial solubilization of inorganic P can occur through acidification via gluconic acid, the production of which requires the specific co-factor pyrroloquinoline-quinone (PQQ). However, bacteria receive little attention in the root economic space (Matthus et al., 2025), and especially in regards to P nutrition. Unraveling how plants integrate both rhizosphere bacteria and AMF to address their P needs may inform strategies to leverage plant-microbe interactions for more sustainable agriculture.

76 AMF colonize plant roots only when the root system is sufficiently developed (Werner & Kiers,
77 2015), whereas P-cycling bacteria are present from early seed germination (Nunes et al.,
78 2022). However, little is known about the enrichment of P-cycling bacteria in the rhizosphere
79 before and after AMF colonization. To address this gap in knowledge, we compared the P-
80 cycling bacterial microbiome between the recently characterized wheat root hair mutant *short*
81 *root hair 1* (*srh1*) and its wild-type background (Tsang et al., 2024). We hypothesized that the
82 wheat root hair mutant enriches P-cycling bacteria to a greater extent than its wild-type
83 background in early development, before the AMF symbiosis is prevalent, to compensate for
84 the lack of root hairs. After the AMF symbiosis is established, we hypothesized that the root
85 hair mutant and the wild-type will have similar bacterial P-cycling levels, due to the
86 dependency on AMF for P nutrition. Furthermore, we hypothesized that we could stimulate
87 the root hair mutant to retain its enriched P-cycling microbiome to later stages of its
88 development by growing the plants in P-depleted conditions. To address these hypotheses,
89 we harvested the root hair mutant and its wild-type background from the field at GS11 and
90 GS13 to capture the response of the P-cycling bacterial community before and after AMF
91 establishment. To evaluate the AMF and bacterial fractions of the P-cycling microbiome at
92 later developmental stages, we harvested a set of plants grown in pots to booting (GS45-47),
93 at which time P uptake is highest in wheat. In this pot-based setup, we could also manipulate
94 the P status of the soil. Long-read 16S ribosomal RNA (rRNA) amplicon sequencing
95 complemented quantitative polymerase chain reaction (qPCR)-based functional analyses of
96 the bacterial microbiome, while AMF were quantified through qPCR and traditional staining.

97

98 ## Materials and Methods

99 ### Plant material

100 The wheat root hair mutant, *srh1,* and its corresponding wild-type line have been characterized
101 in full (Tsang et al., 2024). Briefly, the mutant was identified in a forward screen of an ethyl
102 methanesulfonate-mutated population created in the spring wheat cultivar Cadenza (Krasileva
103 et al., 2017). In the root hair mutant, root hairs initiate but fail to elongate and were measured
104 to be approximately 0.15 mm long compared to the wild-type length of approximately 1.90 mm
105 (Tsang et al., 2024).

106 ### Field experiment set-up and sampling

107 Wild-type and mutant seeds were sown in spring 2024 in a complete randomized block design
108 in Hinxton, Cambridgeshire, United Kingdom (52°05'56.1"N, 0°10'41.8"E). The soil pH, Olsen
109 extractable P, and ammonium nitrate extractable potassium (K) and magnesium (Mg) were
110 measured on unplanted soil by NRM Cawood Scientific (Bracknell, UK) (Table S1).

Approximately 120-180 seeds were sown per plot, where each plot measured 1x1 m with 6 rows of plants per plot. Plants were excavated at GS11 and GS13 (Zadoks et al., 1974) (two and four weeks post-sowing, respectively). One individual plant was sampled from each replicate plot (n = 10) using a sterilized shovel, with care to harvest the entire root system.

Plants were gently shaken to remove the loosely attached bulk soil. The shoot length and the length of the longest root of the root system were measured. The rhizosphere sample (soil influenced by the root) was taken following the procedures described by Guan et al. (2024). Briefly, the roots were placed in 25 mL sterile Milli-Q water and shaken for 30 s; the resulting soil was collected as rhizosphere soil. At each sampling time point, bulk soil (n = 5) was also collected from the bare soil between the plots. The rhizosphere and bulk soil samples were stored at -80 °C until freeze-drying under vacuum at -70 °C. Thereafter, the dried soil samples were stored at 4 °C until subsequent DNA extraction. Shoots were dried at 37 °C, and the shoot dry weight was recorded.

Roots were stored in 70% ethanol at 4 °C prior to root scanning. Root scans were taken using an Epson Dual Lens System Epson Perfection V800 Photo at 600 DPI in greyscale. RhizoVision Explorer version 2.0.3 (Seethepalli et al., 2021) was used to analyze the root scans to calculate total root length, average diameter, perimeter, volume, surface area, and branching frequency. Scans were taken in “Broken roots” mode and at an image thresholding level of 175. Edge smoothing was enabled with a threshold of 3, and root pruning was enabled at a threshold of 10. Non-root objects below 2 mm^2 were removed. After root scanning, the roots were dried at 37 °C, and the dry weight was subsequently recorded.

Pot experiment set-up and sampling

High- and low-P field soil was collected from the Sawyers Experimental Field site at Rothamsted Research (Harpenden, UK; 51° 48′ 59.39″ N, 0° 22′ 33.28″ W). Soils from two historically low-P plots (last measured Olsen P = 7.1 mg/kg and 5.7 mg/kg in February 2022; A. Riche, personal communication, May 1, 2024) and two historically high-P plots (last measured Olsen P = 19.3 mg/kg and 18.6 mg/kg in February 2022; A. Riche, personal communication, May 1, 2024) were collected and mixed to create the low- and high-P potting soil, respectively. The soil was sieved through 4 mm mesh and mixed with washed sand (Horticultural Silver Sand, Melcourt, Tetbury, UK) in a 3:2 ratio (w/w) to improve drainage and root aeration. Samples of the soil-sand mixture were analyzed for pH, Olsen extractable P, and ammonium nitrate extractable potassium (K) and magnesium (Mg) by NRM Cawood Scientific (Bracknell, UK) (Table S1).

Two-liter pots (12 cm H x 12 cm W x 20 cm L) were sterilized (Hortisept Pro, Conka, Nelson, UK), dried, and filled with the soil-sand mixture. Wild-type and mutant seeds (n = 8) were pre-

146 germinated on damp filter paper in the dark for three days before planting one seed per pot.
147 Plants were grown in a climate chamber (Conviron CMP6010) under 16-hour days at 20 °C,
148 60% humidity, and light level 3, followed by 8-hour nights at 18 °C and 60% humidity.
149 Throughout growth, pots were rotated twice a week and watered as needed approximately
150 three times a week. Plants were harvested at booting (GS45-47; Zadoks et al., 1974) after
151 five weeks of growth. The leaf sheath of the plants was swollen and just started to open to
152 expose the ear.

153 Plants were gently removed from the pots, and the root system was divided in half along the
154 longitudinal axis. Approximately half the root system was used for rhizosphere sampling as
155 described in Guan et al. (2024). Briefly, the roots were placed in 25 mL sterile Milli-Q water
156 and shaken for 30 s; the resulting soil was collected as rhizosphere soil. Rhizosphere soil
157 samples were stored at -80 °C until freeze-drying under vacuum at -70 °C. Thereafter, the
158 dried rhizosphere soil samples were weighed as a proxy for rhizosheath size and stored at 4
159 °C until DNA extraction. Shoots were dried at 37 °C and subsequently the dry weight was
160 recorded. Roots were stored in 50% ethanol at 4 °C until AMF quantification.

161 Dried shoots were homogenized and ground using a zirconium ball mill, and the P
162 concentration was determined using the dry ashing method of Saunders & Williams (1955)
163 followed by the molybdate-blue method (Murphy & Riley, 1962) using flow injection analysis
164 (FIAstar 5000 analyzer, Foss, Hillerod, Denmark). Briefly, 100 mg samples were placed in
165 acid-washed crucibles and ashed in a muffle furnace at 550 °C for one hour. The ash was
166 mixed with 50 mL 0.5 M sulfuric acid and shaken overnight at room temperature. Extracts
167 were filtered through ashless filters (Whatman No. 42), and samples were diluted 10X before
168 analysis. Two blanks and one replicate of the standard reference material 1515 (NIST 1991)
169 (Sigma Aldrich, Denmark) were included in the analysis.

170 ### AMF quantification

171 Due to the small and fragile root system of the young plants at GS11 and GS 12-13, relative
172 qPCR was used to quantify AMF colonization (Bodenhausen et al., 2021). DNA was extracted
173 from the dried roots using a FastPrep-24 5G beadbeating system (MP Biomedicals, Irvine,
174 CA, USA) at 6.0 m/s for 40 s and the FastDNA SPIN Kit (MP Biomedicals, Irvine, CA, USA)
175 following the manufacturer's instructions. DNA quality and quantity were recorded using a
176 NanoDrop ND-1000 spectrophotometer (Thermo Fisher Scientific, Carlsbad, CA, USA) and a
177 Qubit 2.0 Fluorometer (Thermo Fisher Scientific, Carlsbad, CA, USA), respectively. DNA was
178 diluted ten-fold to a concentration between 1 and 10 ng/µL. AMF colonization was quantified
179 using the 18S rRNA gene fragment, amplified with the AMF-specific primers AMG1F (Hewins
180 et al., 2015) and AM1 (Helgason et al., 1998) (Table S2) on an AriaMx Real-Time PCR system

181 (Agilent Technologies, Santa Clara, CA, USA) using the PCR conditions described in
182 Bodenhausen et al. (2021). The AMF 18S rRNA gene signal was normalized using a wheat
183 gene encoding a heterogenous nuclear ribonucleoprotein Q, *hn-RNP-Q*, which was amplified
184 with previously described primers (Table S2) and PCR conditions (Qi et al., 2012). For both
185 primer sets, each 20 µL qPCR reaction contained 10 µL 2X Brilliant III Ultra-Fast SYBR Green
186 qPCR Master Mix with Low ROX (Agilent Technologies, Santa Clara, CA, USA), 0.4 µM each
187 of forward and reverse primer, 1 mg/mL bovine serum albumin (New England Bioabs, MA,
188 USA), and 2 µL of template DNA. qPCR products were visualized on a 1% agarose gel using
189 GelRed (Sigma Aldrich, Denmark) to confirm amplification of the target gene. Negative
190 controls were run in triplicate for each primer pair. Raw fluorescence data were imported to
191 LinRegPCR (version 2021.2) (Ruijter et al., 2009) to determine cycle number to threshold (*Ct*)
192 and efficiency (*E*) using the default baseline threshold from LinRegPCR. The AMF 18S rRNA
193 gene signal was normalized to plant DNA using the formula $\frac{E_{hn-RNP-Q}{}^{Ct_{hn-RNP-Q}}}{E_{18S}{}^{Ct_{18S}}}$ as described
194 by Bodenhausen et al. (2021).

195 At booting (GS45-47), AMF colonization was quantified via staining (Phillips & Hayman, 1970).
196 From each plant, approximately 0.2 g of root taken from the middle of the root system was
197 stained with Trypan Blue. Root samples were incubated in 2 mL 10% KOH for 25 min at 90˚C.
198 Subsequently, the KOH was removed, and the roots were washed twice with distilled water.
199 After washing, roots were incubated in 2 mL 0.3 M HCl for 30 min at room temperature. After
200 removing the HCl, roots were incubated in 2 mL 0.1% Trypan Blue stain for eight minutes at
201 90˚C. Roots were then washed twice with acidic glycerol (1:1 glycerol:0.3 M HCl v/v) and
202 incubated with the last wash overnight at room temperature in the dark. At least ten stained
203 root sections measuring approximately 1 cm per sample were mounted on microscope slides.
204 Scoring for AMF presence and arbuscule formation was performed on 100 fields of view per
205 slide using a Leica DMLS microscope (Leica Microsystems, Wetzlar, Germany) under 200X
206 magnification (Brundrett et al., 1996).

207 Bacterial P-cycling gene quantification and 16S rRNA gene amplicon sequencing

208 DNA from up to 500 mg freeze-dried rhizosphere samples was extracted using a FastPrep-24
209 5G beadbeating system (MP Biomedicals, Irvine, CA, USA) at 6.0 m/s for 40 s and the
210 FastDNA SPIN Kit for soil (MP Biomedicals, Irvine, CA, USA) following the manufacturer's
211 instructions. DNA quality and quantity were tested using a NanoDrop ND-1000
212 spectrophotometer (Thermo Fisher Scientific, Carlsbad, CA, USA) and a Qubit 2.0
213 Fluorometer (Thermo Fisher Scientific, Carlsbad, CA, USA), respectively. DNA was diluted
214 ten-fold to a quantity between 1 and 10 ng/µL.

215 Quantification of the 16S rRNA gene and bacterial P-cycling genes (*bpp*, *phnK*, *phoD*, *phoX*,
216 and *pqqC*) in the rhizosphere samples was performed via qPCR using the AriaMx Real-Time
217 PCR system (Agilent Technologies, Santa Clara, CA, USA) following the qPCR conditions
218 described in Hao et al. (2020) and primers in Table S2. qPCR products were visualized on a
219 1% agarose gel using GelRed (Sigma Aldrich, Denmark) to confirm amplification of the target
220 gene. Standard curves and negative controls were run in triplicate on each plate. Abundance
221 of the P-cycling genes was normalized to 16S rRNA copies.

222 The bacterial community in the rhizosphere was analyzed by sequencing 1050 bp of the 16S
223 rRNA gene, amplified using primers 341F (5'- CCTACGGGNGGCWGCAG -3') and 1391R (5'-
224 GACGGGCGGTGWGTRCA -3') (Thijs et al., 2017) with the Platinum SuperFi II polymerase
225 (Thermo Fischer Scientific, Waltham, USA). The ZymoBIOMICS Microbial Community DNA
226 Standard (Zymo Research, Irvine, CA, USA) was included as a sequencing control. The PCR
227 cycling conditions were as follows: an initial denaturation step of 98 °C for 30 s, followed by
228 30 cycles of denaturation at 98 °C for 10 s, annealing at 64 °C for 30 s, and elongation at 72
229 °C for 45 s, and a final elongation at 72 °C for 5 min. PCR products were visualized via
230 electrophoresis on a 1% agarose gel before purification using AMPure XP beads (Beckman
231 Coulter Inc., Brea, CA, USA) at a 0.6 ratio. The sequencing library was prepared using a native
232 barcoding kit V14 (SQK-NBD114.96) and sequenced using a PromethION R10.4.1 flow cell
233 on the PromethION P2 Solo platform (Oxford Nanopore, UK).

234 Adapter trimming and basecalling were performed using Dorado version 0.7.0 using the super
235 accurate setting (github.com/nanoporetech/dorado). Seqtk (github.com/lh3/seqtk) was used
236 to discard reads below 1000 bp and above 1500 bp. Amplicon sequences were extracted from
237 between the primer sequences using the script strip_degen_primer_deep
238 (github.com/padbr/asat). NanoFilt version 2.8.0 (De Coster et al., 2018) was used to discard
239 amplicon sequences with an average quality score below 25. Cutadapt version 3.5 (M. Martin,
240 2011) was used to truncate longer reads at 1010 bp. The remainder of the analysis was
241 performed in R version 4.3.1 (R Core Team, 2023). The reads were dereplicated to form
242 amplicon sequence variants (ASVs) and assigned taxonomy using dada2 version 1.22.0
243 (Callahan et al., 2016) with the SILVA database version 138.2 (Quast et al., 2013). The ASV
244 table was transformed to a phyloseq object for subsequent analysis using phyloseq version
245 1.44.0 (McMurdie & Holmes, 2013). Non-bacterial ASVs and those assigned to chloroplasts
246 and mitochondria were discarded before the ASVs were agglomerated at the genus level while
247 retaining non-classified reads. The ZymoBIOMICS Microbial Community DNA Standard
248 (Zymo Research, Irvine, CA, USA) was used to assess sequencing contamination. Ampvis2
249 version 2.8.1 (Andersen et al., 2018) was used to visualize bacterial community composition.
250 A dissimilarity matrix was calculated with rarefaction to 6639 reads using avgdist from the

251 vegan package version 2.6-4 with default parameters (vegandevs.github.io/vegan) and was
252 used to generate the principal coordinate analysis based on Bray-Curtis dissimilarities and to
253 run a PERMANOVA using adonis2 from vegan. Pairwise comparisons were made with the
254 package pairwiseAdonis version 0.4.1 (github.com/pmartinezarbizu/pairwiseAdonis). The
255 Shannon diversity index (alpha diversity) was calculated 100 times, as proposed by Schloss
256 (2024). Briefly, the dataset was rarefied to 6639 reads, and the Shannon diversity index was
257 subsequently calculated as the mean Shannon diversity index over 100 replicates.
258 Differentially abundant ASVs between the mutant and wild-type were generated using corncob
259 version 0.4.1 (B. D. Martin et al., 2020) with a false discovery rate of 0.05.

260 Raw reads are deposited in NCBI under BioProject PRJNA1308004.

261 Statistical analysis

262 Data analysis was conducted in R version 4.3.1 (R Core Team, 2023), and all plots were
263 created using ggplot2 version 3.5.1 (Wickham, 2016). Significance was defined as $p < 0.05$.
264 When comparing means, the Shapiro-Wilk test was used to check for normality. The Student's
265 t-test was used to compare means for parametric groups, while the Wilcoxon test was used
266 for non-parametric groups. All qPCR data were log-transformed before analysis, and due
267 to heteroscedasticity and different data structures across growth stages, separate models
268 were made for each gene in each growth stage. All analyses of variance (ANOVAs) were
269 performed using the car package version 3.0-5 (Fox & Weisberg, 2019). All post-hoc pairwise
270 comparisons were performed using the emmeans package version 1.10.4
271 (rvlenth.github.io/emmeans) with Tukey's Honestly Significant Difference (HSD) test.

272 Results

273 Loss of root hair elongation impacts wheat development across growth stages.

274 We initially evaluated the effect of the *srh1* mutation, which arrests root hair elongation
275 (Tsang et al., 2024), on overall plant performance in real soils across three growth stages:
276 first leaf fully unfolded (GS11), three leaves unfolded (GS13), and booting (GS45-47). At the
277 two youngest growth stages, aboveground growth was no different between the two
278 genotypes; the root hair mutant had longer shoots at GS11 (Student's t-test, $p < 0.05$), but
279 this was not reflected in shoot biomass (Student's t-test, $p > 0.05$, Figure 1A-B). On the other
280 hand, root growth was stunted in the root hair mutant at GS11 but restored at GS13 (Figure
281 S1). The lack of root hair elongation restricted rhizosheath development across the growth
282 stages (Student's t-test, $p < 0.05$), although this was obscured at GS13 due to wet soils at
283 harvest and enlarged rhizosheath size (Figure 1C).

At booting (GS45-47), the phenotypic difference between the genotypes was apparent. The root hair mutant was stunted in aboveground growth compared to the wild-type (Student's t-test or Wilcoxon test, $p < 0.05$, Figure 1A-B). However, shoot P concentration at this growth stage was not different between the root hair mutant (2.84 mg/g ± 0.374 mg/g) and the wild-type (2.47 mg/g ± 0.246 mg/g) (Wilcoxon test, $p > 0.05$).

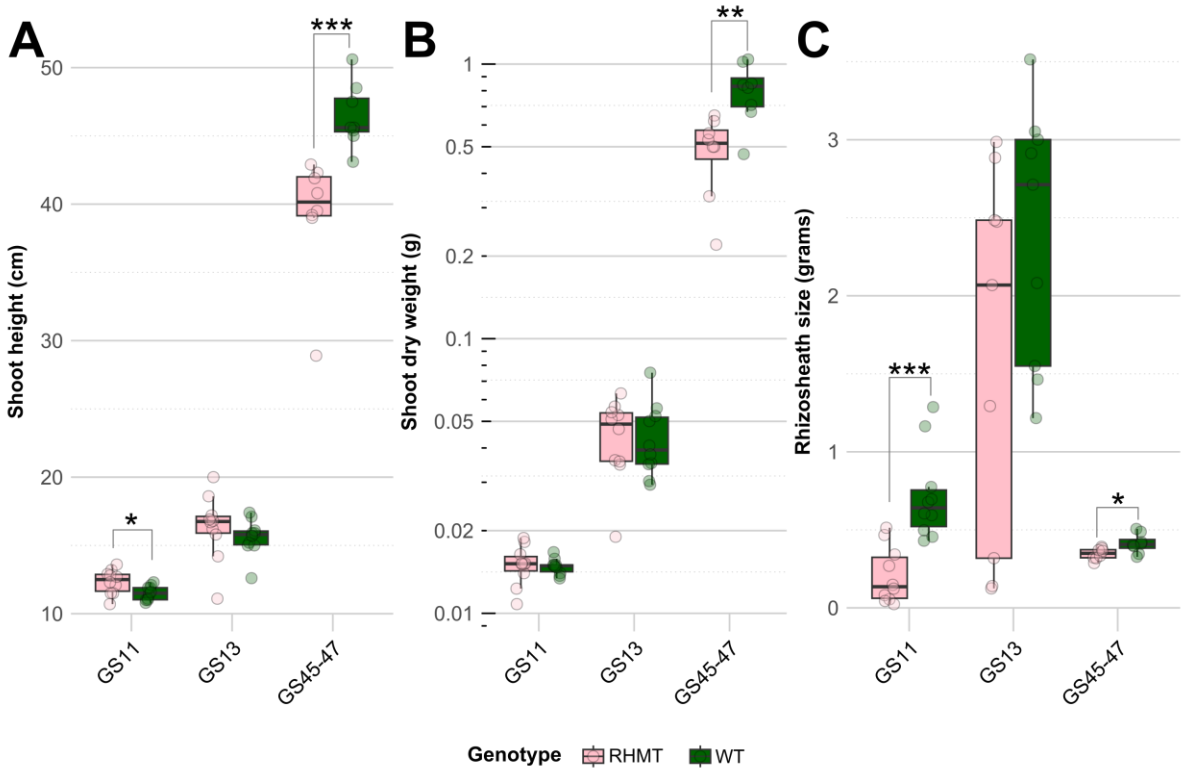

Figure 1. Plant performance of the root hair mutant (RHMT) and wild-type (WT), measured as shoot height (A), shoot dry weight (B), and rhizosheath size (C) across growth stages. Genotypes were compared within each growth stage using t-tests (parametric data) or Wilcoxon tests (non-parametric data). *$p < 0.05$, **$p < 0.01$, ***$p < 0.001$.

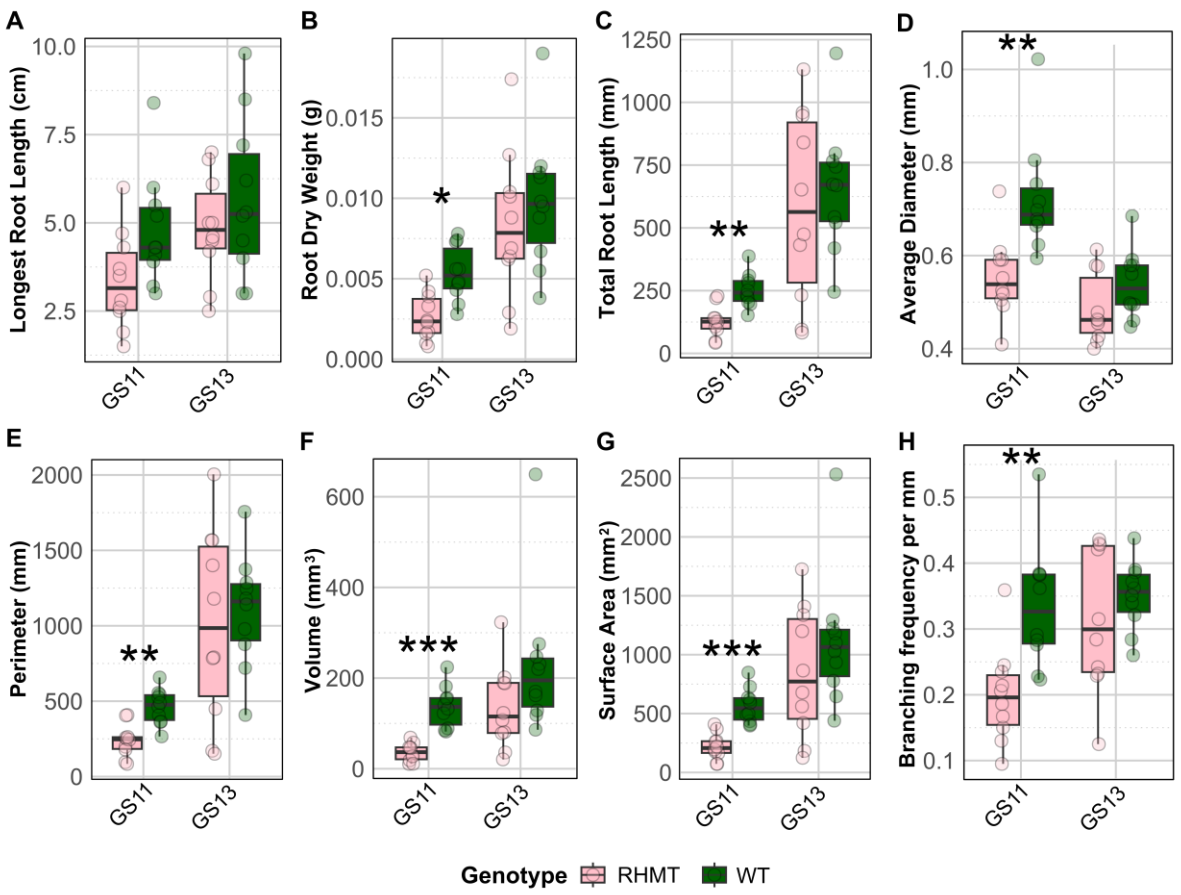

Supplemental Figure 1. Root phenotypic data of the root hair mutant (RHMT) and wild-type (WT) across the first two growth stages. Genotypes were compared within each growth stage using t-tests (normal data) or Wilcoxon tests (non-normal data). *p < 0.05, **p < 0.01, ***p < 0.001.

Initial higher colonization of bacteria harboring P mineralization genes in the wheat root hair mutant.

The ability of the root hair mutant to enrich its bacterial microbiome for P-cycling was assessed alongside the development of the AMF symbiosis across the three growth stages.

At GS11, the relative abundance of all bacterial P-cycling genes, except for *phoX*, was affected by sample source (root hair mutant, wild-type, or bulk soil) at GS11 (one-way ANOVA, $p < 0.05$, Table S3). Bacterial genes involved in organic P mineralization (*bpp*, *phnK*, and *phoD*) were enriched in the rhizosphere of the root hair mutant compared to the wild-type (Tukey's HSD, $p < 0.05$, Table 1). No differences in the relative abundance of *phoX* (periplasmic phosphatase) and *pqqC* (pyrroloquinoline-quinone synthase) were found between the root hair mutant and wild-type (Tukey's HSD, $p > 0.05$). There was low AMF signal in both root hair mutant and wild-type plants, and the log2 ratio of AMF DNA to plant DNA was below zero.

312 There was no enrichment of AMF signal in either genotype (Figure 2, two-way ANOVA, $p >$
313 0.05, Table S4).

314 At GS13, the relative abundance of *bpp*, *phnK,* and *phoD* in the rhizosphere of the root
315 hair mutant decreased to the level of the wild-type. While sample source exhibited an effect
316 on gene relative abundance (one-way ANOVA, $p < 0.05$, Table S3), with the exception of *phoD*
317 and *phoX*, this was driven by the difference in gene abundance between the plant
318 rhizospheres and bulk soil (Table 1). The decrease in P mineralization gene relative
319 abundance coincided with an increase in AMF signal across the plants at this growth stage.
320 The ratio of AMF DNA to plant DNA increased and was higher than at GS11, indicating the
321 establishment of the AMF symbiosis (Figure 2; two-way ANOVA, $p < 0.05$, Table S4), but there
322 was no effect of genotype on AMF signal (two-way ANOVA, $p > 0.05$, Table S4).

323 At the latest growth stage, GS45-47, there was no enrichment of bacterial P-cycling genes in
324 the root hair mutant compared to the wildtype, similar to GS13 (Table 1, Tukey's HSD, $p >$
325 0.05). Only the bulk soil was different from the plant rhizospheres for the genes *phoD*, *phoX*,
326 and *pqqC* (Tukey's HSD, $p < 0.05$). On the other hand, microscopy indicated increased total
327 AMF colonization in the root hair mutant compared to the wild-type (Figure 2, Wilcoxon test, p
328 < 0.05). Arbuscule formation reflected the result of total colonization, with the mutant exhibiting
329 elevated arbuscule formation compared to the wild-type (Figure 2, Wilcoxon test, $p < 0.05$).

330 In summary, the results showed that at early stages of plant growth prior to AMF root
331 colonization, a higher abundance of bacteria involved in P mineralization colonized the
332 rhizosphere of the root hair mutant compared to the wild-type. This phenomenon was no
333 longer observed upon establishment of AMF symbiosis, and bacterial P cycling genes were
334 no longer enriched in the root hair mutant rhizosphere.

335

Growth stage	Sample Source	*bpp*	*phnK*	*phoD*	*phoX*	*pqqC*
GS11	RHMT	1.14e-03 ± 7.05e-04 a	2.52e-01 ± 1.91e-01 a	2.77e-01 ± 2.56e-01 a	4.03e-02 ± 1.05e-02 a	3.75e-03 ± 2.83e-03 a
GS11	WT	5.73e-04 ± 1.17e-04 b	1.21e-01 ± 2.32e-02 b	7.75e-02 ± 9.24e-03 b	4.28e-02 ± 7.21e-03 a	1.83e-03 ± 3.74e-04 a
GS11	Bulk soil	5.09e-04 ± 1.01e-04 b	1.1e-01 ± 2.92e-02 b	1.05e-01 ± 2.27e-02 ab	5.72e-02 ± 1.85e-02 a	6.42e-03 ± 2e-03 b
GS13	RHMT	7.54e-04 ± 3.05e-04 a	1.61e-01 ± 9.2e-02 a	1.14e-01 ± 1.51e-01 a	4.92e-02 ± 1.23e-02 a	2.17e-03 ± 1.39e-03 a
GS13	WT	6.08e-04 ± 1.82e-04 a	1.17e-01 ± 3.58e-02 ab	6.86e-02 ± 2.02e-02 a	4.08e-02 ± 1.58e-02 a	1.67e-03 ± 6.39e-04 a
GS13	Bulk soil	4.08e-04 ± 1.59e-04 b	8.31e-02 ± 2.14e-02 b	8.09e-02 ± 2.13e-02 a	4.75e-02 ± 1.78e-02 a	5.02e-03 ± 1.75e-03 b

GS45-47	RHMT	2.18e-04 4.12e-05	± a	1.45e-01 4.30e-02	± a	6.26e-02 1.57e-02	± a	3.24e-02 1.06e-02	± a	5.19e-03 2.33e-03	± a
GS45-47	WT	2.70e-04 3.72e-05	± a	1.81e-01 3.40e-02	± a	6.85e-02 1.72e-02	± a	4.02e-02 1.42e-02	± a	5.47e-03 1.94e-03	± a
GS45-47	Bulk soil	2.31e-04 6.75e-05	± a	1.71e-01 7.06e-02	± a	4.66e-01 1.49e-01	± b	2.00e-03 1.03e-03	± b	2.68e-03 1.02e-03	± b

Table 1. Relative abundance of bacterial P-cycling genes in root hair mutant (RHMT) and wild-type (WT) rhizosphere. Relative abundance was calculated by normalizing against 16S rRNA gene copies, and the mean is presented ± the standard deviation. Log-transformed gene relative abundance was compared among genotypes within each growth stage using one-way ANOVA with Tukey's HSD post-hoc test. Means that share the same letter are not statistically different ($p < 0.05$).

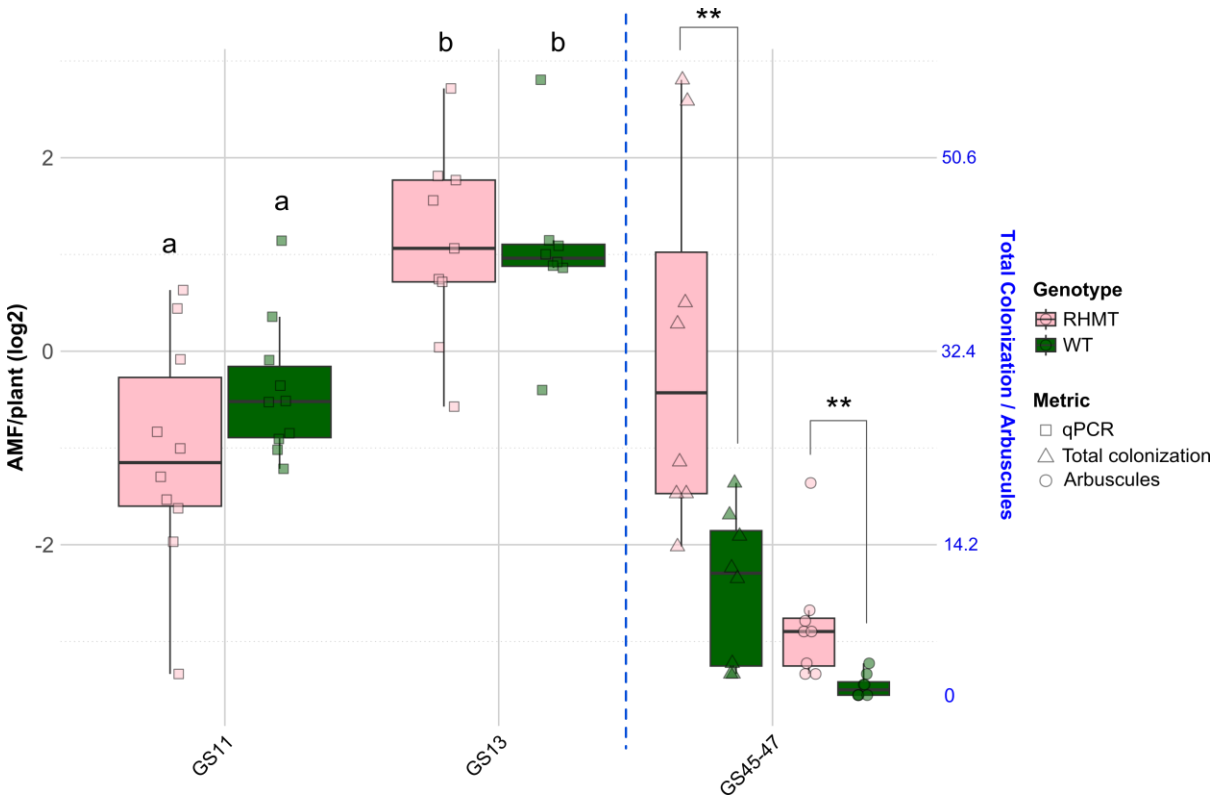

Figure 2. AMF signal in the root hair mutant (RHMT) and wild-type (WT) quantified via qPCR or via microscopy (percent total colonization and percent arbuscule formation) across the growth stages. The boxplots display the median, the two hinges (25th and 75th percentile), and the upper and lower whiskers (extending to the largest and smallest values no further than 1.5 times the interquartile range). True data points are overlaid on the boxplots as filled circles. qPCR means were compared using one-way ANOVA with Tukey's HSD post-hoc test; means that share the same letter are not statistically different ($p < 0.05$). Microscopy means (percent total colonization and arbuscule formation) were compared with Wilcoxon test. **$p < 0.01$.

353

354 Loss of root hair elongation had minor effects on bacterial taxonomic composition in the
355 rhizosphere across development.

356 To reveal the differences in rhizosphere bacterial community composition between the root
357 hair mutant and the wild-type, long-read 16S rRNA amplicon sequencing was performed on
358 the rhizosphere of the plants across the three growth stages. After filtering, 1,264,834 reads
359 were retained. The median number of reads per sample was 14,570. 80% of the ASVs were
360 identified at genus level.

361 Across the three growth stages, genera such as *Bacillus, Niallia, and Flavobacterium* were
362 most abundant in both root hair mutant and wild-type plants (Supplemental Figure S2). There
363 was no effect of root hair elongation on the alpha diversity of the bacterial microbiome in the
364 rhizosphere across the three growth stages (Supplemental Figure S2, Wilcoxon test, $p > 0.05$).

365 No bacterial genera were differentially enriched in either genotype at GS11. On the other hand,
366 at GS13, *Arthrobacter*, *Ensifer*, *Pseudomonas*, *Stenotrophomonas*, *Pedobacter*, and *Pantoea*
367 were enriched in the root hair mutant, while *Ilumatobacter* and an unidentified genus of the
368 Fibrobacteraceae family were enriched in wild-type plants (Figure 3A). At GS45-47, only an
369 unclassified genus of the Mycoplasmataceae family was enriched in the root hair mutant
370 (Figure 3B).

371 In summary, the loss of root hair elongation had limited impact on the bacterial community in
372 the wheat rhizosphere, with GS13 being the most affected by the mutation.

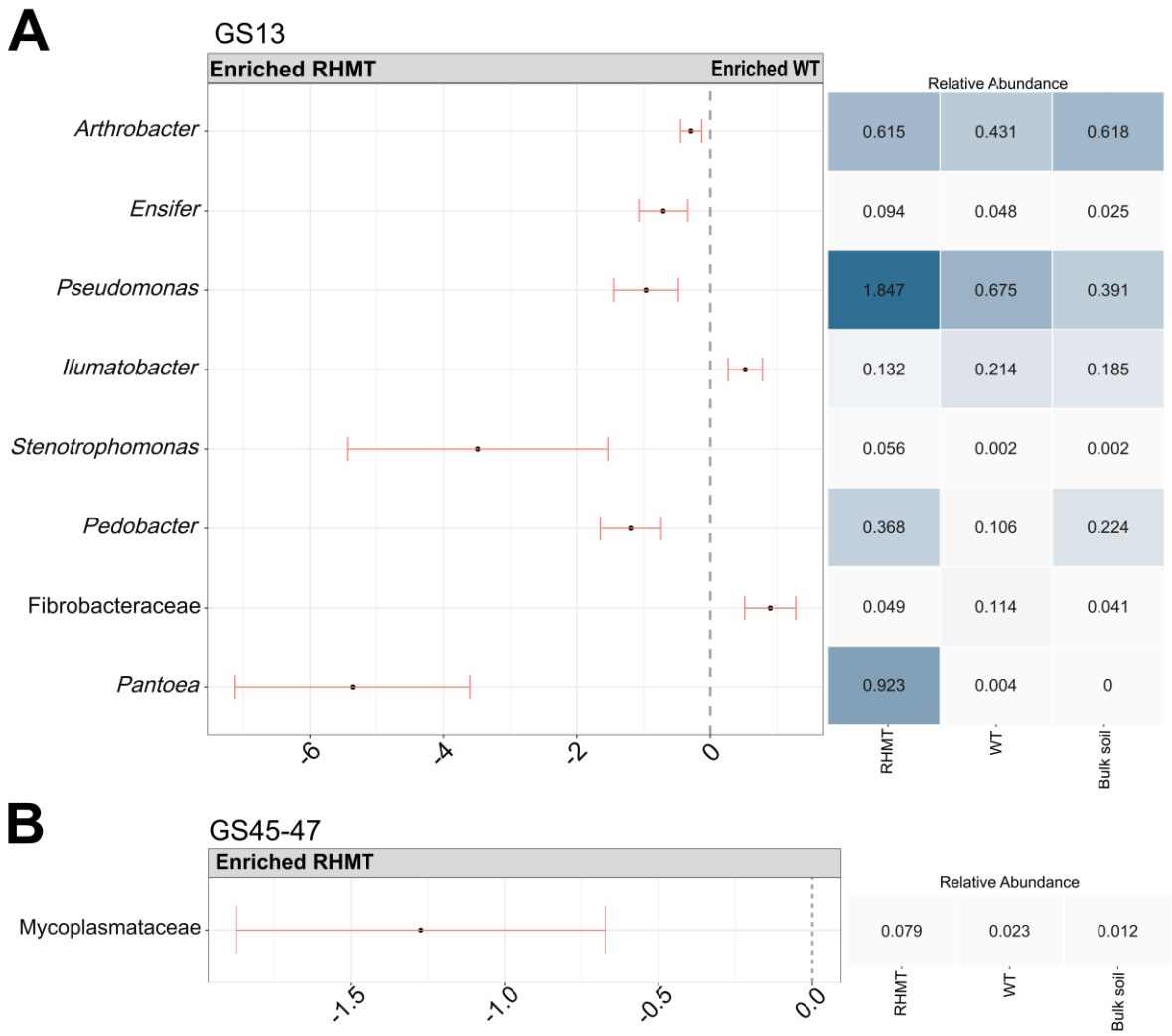

Figure 3. Taxa enriched in the root hair mutant (RHMT) versus the wild-type (WT) across growth stages. At GS11, there were no differentially abundant genera. The differential abundance between the RHMT and WT was determined using beta-binomial regression with corncob. Only taxa that had a $p < 0.05$ after correcting for multiple testing (FDR) were considered significant. The heatmap displays the mean relative abundances of the taxa in the RHMT, WT, or bulk soil samples.

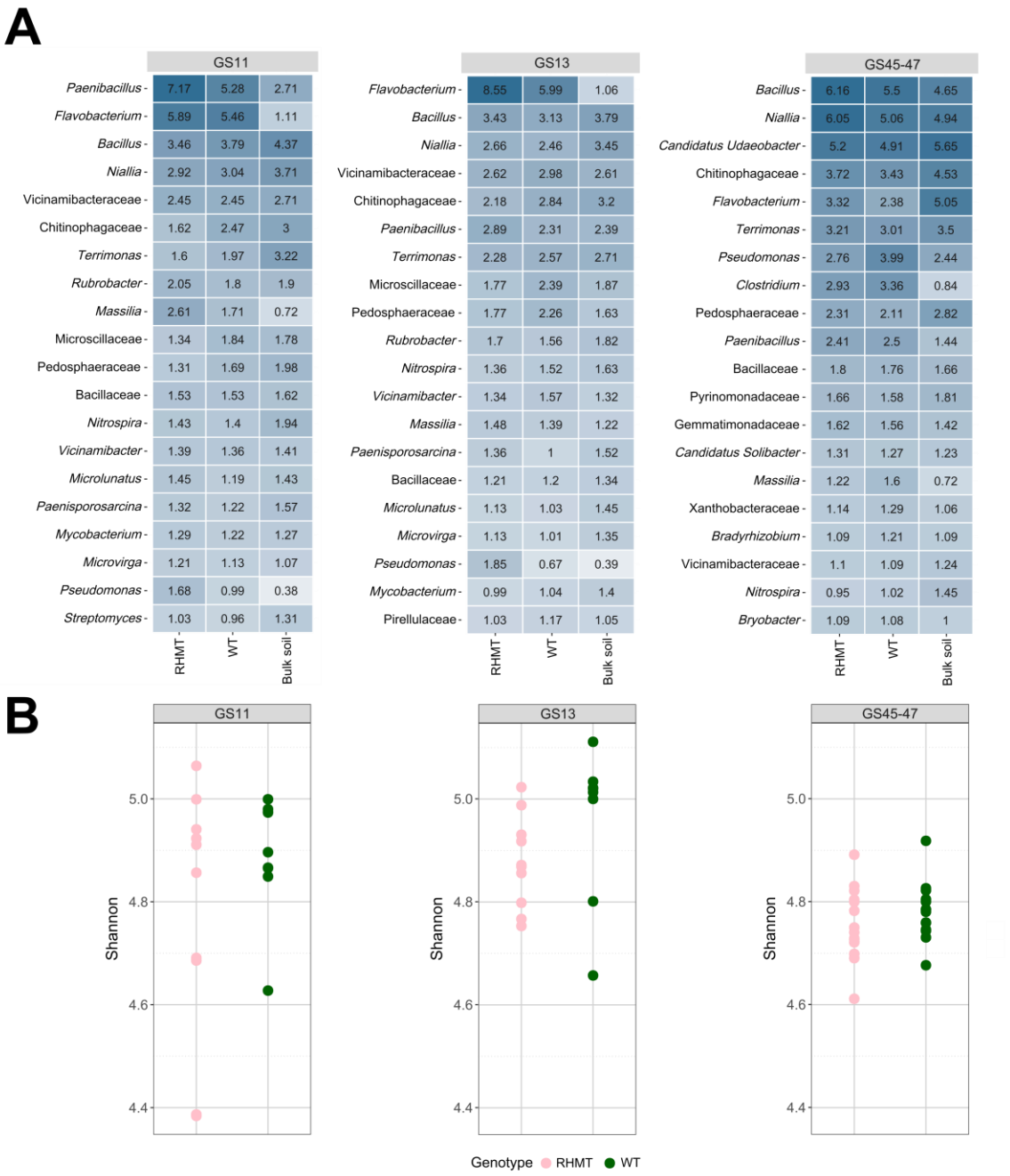

Supplemental Figure S2. Rhizosphere bacterial community composition of the root hair mutant (RHMT) and wild-type (WT) across growth stages. (A) The heatmap displays the mean relative abundances of the taxa in the RHMT, WT, or bulk soil samples. (B) Alpha diversity as described by the Shannon diversity index across growth stages in the RHMT and WT. Each point represents a sample. Genotypes were compared within each growth stage using t-tests (normal data) or Wilcoxon tests (non-normal data). *p < 0.05.

388 Low-P soil status enriches arbuscule formation and not bacterial P mineralization in
389 response to loss of root hair elongation.

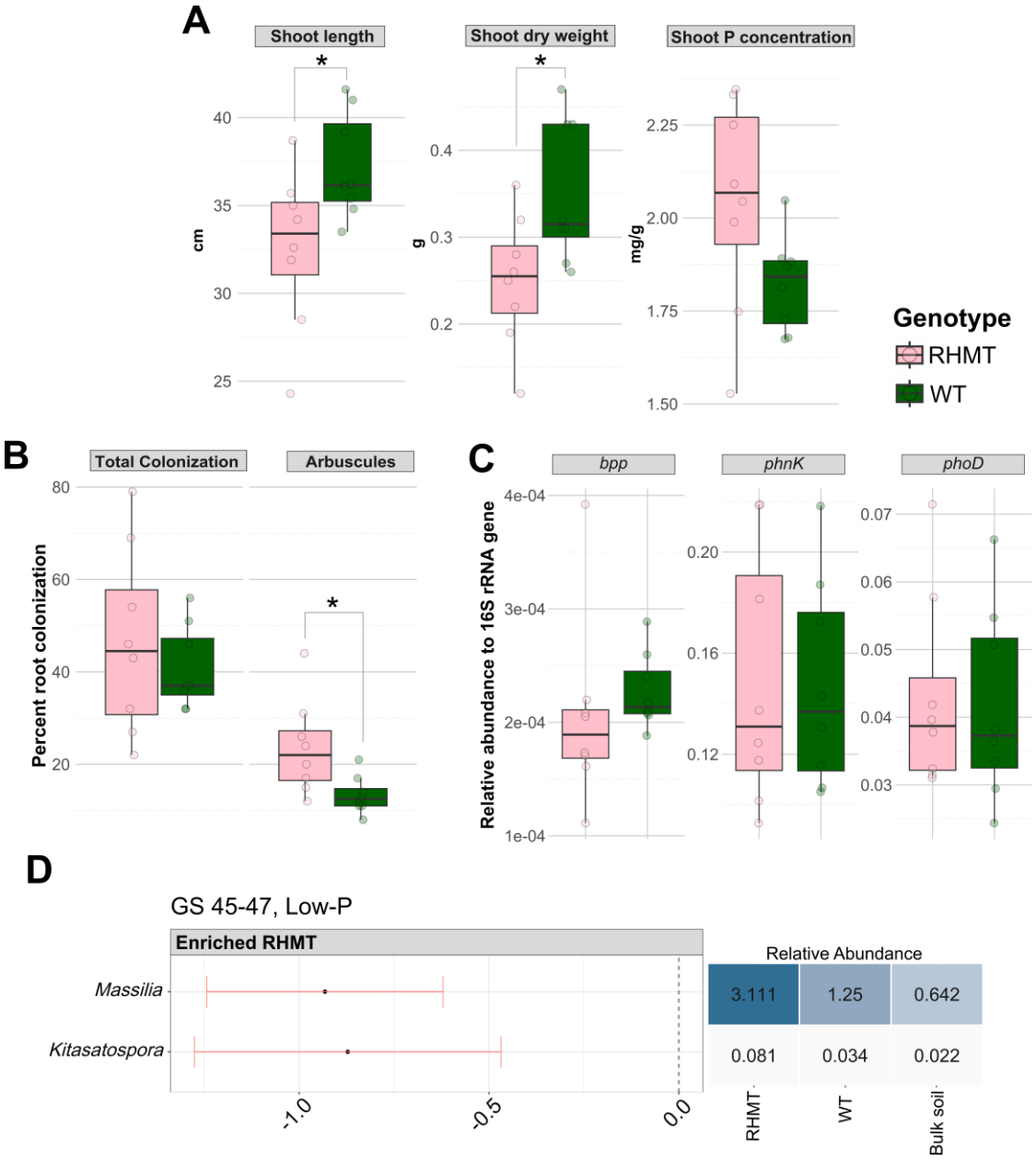

390

391 **Figure 4. Response of the root hair mutant (RHMT) and wild-type (WT) to low-P**
392 **conditions at GS45-47.** (A) Plant performance as measured by aboveground biomass and
393 shoot P concentration. (B) AMF total colonization and arbuscule formation. (C) Relative
394 abundance of bacterial P mineralization genes. (D) Differentially abundant bacterial genera
395 between the root hair mutant and wild-type. The differential abundance was determined using
396 beta-binomial regression with corncob. Only genera that had a $p < 0.05$ after correcting for
397 multiple testing (FDR) were considered significant. The heatmap displays the mean relative
398 abundances of the genera in the RHMT, WT, or bulk soil samples. The boxplots display the
399 median, the two hinges (25th and 75th percentile), and the upper and lower whiskers

400 (extending to the largest and smallest values no further than 1.5 times the interquartile range).
401 True data points are overlaid on the boxplots as filled circles. Means were compared with the
402 Wilcoxon test. *$p < 0.05$.

403

404 To stimulate the root hair mutant to retain P-cycling bacteria further along in its development,
405 we grew the plants to booting (GS45-47) in P-depleted soil. The root hair mutant and wild-type
406 were grown in pots using soil from a historically low-P fertilized plot from a nutrient depletion
407 field trial. In the low-P soil, both genotypes grew only half the biomass compared to when the
408 plants were grown in soil from the P-replete plots of the nutrient depletion field trial (Figure 1
409 and Figure 4A). The root hair mutant also grew smaller shoots compared to the wild-type in
410 the low-P soil (Figure 4A, Wilcoxon test, $p < 0.05$). Shoot P concentration of the two genotypes
411 was not different in the low-P soil (Figure 4A, Wilcoxon test, $p > 0.05$).

412 While the two genotypes were colonized equally by AMF in the low-P soil, the root hair mutant
413 demonstrated higher arbuscule formation (Willcoxon test, $p < 0.05$) (Figure 4B). The bacterial
414 P mineralization genes that were enriched in the root hair mutant at early seedling growth
415 under P-replete conditions (Table 1) were not enriched under low-P conditions at GS45-47
416 (Figure 4C). There was an effect of sample source (root hair mutant, wild-type, or bulk soil) on
417 gene relative abundance (one-way ANOVA, $p < 0.05$, Table S5), but there were no bacterial
418 P-cycling genes enriched in the root hair mutant compared to the wild-type in low-P conditions
419 (Tukey's HSD, $p > 0.05$, Table S6).

420 Soil P status influenced the bacterial microbiome community structure in the rhizosphere
421 (PERMANOVA, $p = 0.001$, $R2 = 0.36$), as did the interaction between genotype and soil P
422 status (PERMANOVA, $p = 0.014$, $R2 = 0.07$) (Figure S3). Despite this, only two genera,
423 *Massilia* and *Kitasatospora*, were enriched in the root hair mutant under low-P (Figure 4D),
424 and there was no difference in alpha diversity between the two genotypes (Figure S3,
425 Student's T test, $p > 0.05$).

426 In summary, low-P conditions did not increase recruitment of bacterial P-cycling genes in the
427 rhizosphere of the root hair mutant at GS45-47, despite the high P demand at this growth
428 stage. During this growth stage, arbuscule formation was enriched in the root hair mutant
429 under low-P.

430

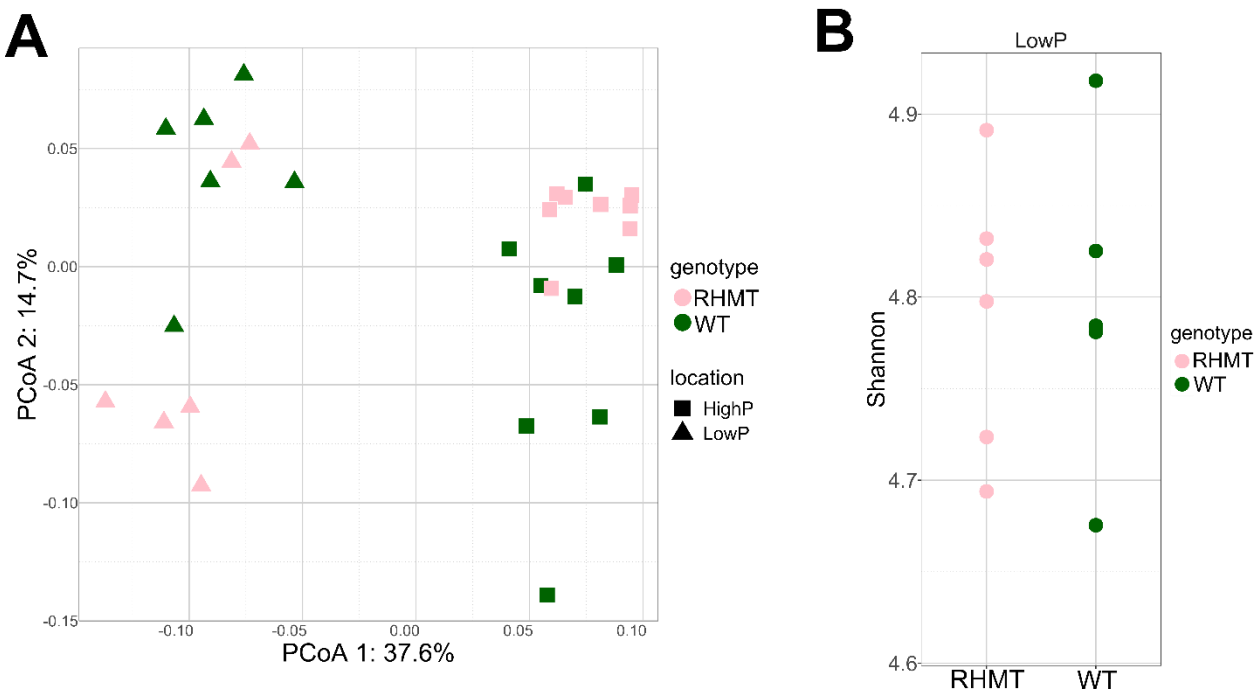

Supplemental Figure S3. Bacterial community composition of the rhizosphere of the root hair mutant (RHMT) and wild-type (WT) under high- and low-P soil conditions. (A) Principal coordinate analysis (PCoA) plot based on Bray-Curtis dissimilarities. Each point represents a sample. (B) Alpha diversity as described by the Shannon diversity index. Each point represents a sample.

Discussion

The potential of the plant to utilize both the bacterial and fungal fraction of the rhizosphere microbiome for P nutrition has yet to be fully understood. We lack knowledge on the modulation of the P-cycling bacterial community in wheat and how this might be contextualized with regards to AMF, the fungal community vital for plant P nutrition (Smith & Smith, 2011). In this work, we used a recently characterized root hair mutant in wheat (Tsang et al., 2024) to induce a limitation in P uptake (Gahoonia et al., 2001) that can be alleviated by the bacterial microbiome (Zhang et al., 2025). Our results provide novel insights on the importance of bacteria and AMF in compensating for the loss of root hair elongation during wheat development and in P-depleted soils.

With regards to plant development, we found a stunting effect of the *srh1* mutation on early root system development in soil, which was mirrored by diminished aboveground biomass at booting (GS45-47). Reduced root growth is typical of hairless mutants in other crop species grown in soil, highlighting the importance of root hairs in overall crop development (Suzuki et al., 2003; Haling et al., 2013; Ma et al., 2020). Rhizosheath size was also reduced in the root

453 hair mutant, in accordance with previous results on the importance of root hairs on root-soil
454 contact (Haling et al., 2013). Despite potential pleiotropic effects of the *srh1* mutation on crop
455 growth, the inhibition of root hair elongation in the mutant is a useful tool to test our hypotheses
456 on microbiome modulation as a response to the absence of root hair elongation.

457 In agreement with our first hypothesis, we demonstrated that the bacterial rhizosphere
458 microbiome of the root hair mutant is enriched with P mineralization genes *(bpp, phoD,* and
459 *phnK*) at GS11. Relative abundance of the P solubilization marker gene *pqqC*, the co-factor
460 for gluconic acid production (An & Moe, 2016), was not different between the root hair mutant
461 and wild-type. Since plants rely on root hairs to mobilize organic P into orthophosphate anions
462 (Gahoonia et al., 2001; Richardson et al., 2011; Ma et al., 2020), the specific enrichment of
463 bacterial organic P mineralization genes in the root hair mutant suggests a bacterial route for
464 organic P acquisition to compensate for the loss of root hairs before the AMF symbiosis is
465 established. Indeed, bacteria that metabolize plant root exudates play a significant role in
466 organic P mineralization in the soil (Wang et al., 2025), indicating a potential relationship
467 between microbial function and plant needs. While we cannot rule out competition for P
468 between bacteria and the plant (Raymond et al., 2021), the specific enrichment of
469 mineralization genes may indicate a beneficial relationship over competition.

470 Our second hypothesis suggested that enrichment of P-cycling genes in the root hair mutant
471 would decrease after AMF symbiosis. Harvest at GS13 revealed that the relative abundance
472 of organic P mineralization genes in the root hair mutant rhizosphere decreased to match that
473 of the wild-type, confirming our hypothesis. This loss of bacterial P mineralization genes at
474 GS13 in the root hair mutant coincided with a marked increase in AMF signal in both genotypes
475 from GS11 to GS13. This aligns with previous work that found AMF colonization in field-grown
476 wheat was absent until GS12 (Marrassini et al., 2024), as the root system required sufficient
477 development prior to initiation of AMF symbiosis (Werner & Kiers, 2015). We also observed
478 that root growth of the mutant, which was stunted in comparison to the wild-type at GS11,
479 increased to match that of the wild-type at GS13. This potentially indicated maturity for AMF
480 colonization or, alternatively, a direct root response to AMF colonization (Zhu et al., 2025).
481 While P uptake in the first weeks of growth plays a vital role in seedling establishment and
482 vigor (Yi et al., 2023), the rate of P uptake in wheat reaches its maximum during booting (Jones
483 et al., 2024). Still, at this late growth stage, the relative abundances of all bacterial P-cycling
484 genes were no different between the mutant and wild-type, while AMF colonization and
485 symbiosis was higher in the root hair mutant. In the absence of root hair elongation, AMF total
486 colonization and arbuscule formation increased, aligning with similar results found in root hair
487 mutants of maize and barely (Jakobsen et al., 2005; Kumar et al., 2019; Ma et al., 2020).
488 Despite the loss of root hairs, which constrains plant P nutrition (Gahoonia et al., 2001), the

489 shoot P concentration was unaffected, indicating dominance of AMF for mineral P uptake.
490 These findings mirrored those found in maize (Kumar et al., 2019).

491 The time series data across three growth stages in wheat indicated a temporal shift from
492 enrichment of bacterial P-cycling to the dominance of the AMF symbiosis in the absence of
493 root hair elongation. We propose that before the AMF symbiosis is fully dominant, wheat can
494 recruit and rely on bacterial P mineralization to meet their P needs. Once the AMF symbiosis
495 is established, the recruitment of these bacteria is no longer prioritized. Quantifying the plant
496 P stress response across developmental stages, when the crop is grown only with its bacterial
497 rhizosphere microbiome or only in the presence of AMF, would clarify the importance of these
498 microbial fractions in wheat P nutrition. However, since two different soils were used for early
499 and late harvest in this work, direct comparisons of the bacterial P mineralization response to
500 the loss of root hair elongation between these experiments must be carefully interpreted.
501 Ideally, measurements of organic P across the growth stages would provide further insights
502 into how soil organic P conditions may influence the responsiveness of organic P
503 mineralization genes in the rhizosphere of the root hair mutant. The AMF communities,
504 colonization potential, and responsiveness may also be different between the field and the
505 pots (Jansa et al., 2014), and direct parallels between the experiments should be interpreted
506 with restraint.

507 Alongside functional profiling, long-read 16S rRNA amplicon sequencing revealed the specific
508 taxa responding to the loss of root hair elongation across the three growth stages. However,
509 there was little overlap between the qPCR data and community structure. That is, P-cycling
510 genes only differed between the youngest plants (GS11), while community composition only
511 differed between older plants (GS13 and GS45-47). This disparity was likely due to 16S rRNA
512 sequences that poorly represent functional capabilities (Jaspers & Overmann, 2004), which
513 we have found to be the case for wheat rhizosphere *Pseudomonas* isolates (Herms et al.,
514 2025). Thus, taxonomic profiling is insufficiently sensitive to reveal P-cycling capabilities, and
515 we therefore prioritize the results of the qPCR analyses for interpretation of P-cycling.
516 Nevertheless, we provide evidence for the role of root hairs in shaping the bacterial community
517 in the wheat rhizosphere. We found that the root hair mutant enriched more bacterial taxa
518 compared to its wild-type, as found in barley (Robertson-Albertyn et al., 2017), while maize
519 had an opposite trend (Quattrone et al., 2024). Only one taxon, Actinomycetales, was similarly
520 enriched across wheat and barley root hair mutants (Robertson-Albertyn et al., 2017). Root
521 hair mutants in wheat and maize both enrich the genus *Stenotrophomonas* (Quattrone et al.,
522 2024). *Stenotrophomonas* is a plant-associated bacterium that might play a role in disease
523 suppression, growth promotion, and nutrient acquisition (Kumar et al., 2023). The disruption
524 in microbiome composition in response to the loss of root hair elongation could be attributed

525 to the loss of unique colonization niches (Buddrus-Schiemann et al., 2010; Mousa et al., 2016)
526 or altered root exudate profiles (Quattrone et al., 2024). Analysis of the root exudates of the
527 wheat root hair mutant, while out of scope in this work, could help further clarify the dysbiosis.

528 Our third hypothesis predicted that we could stimulate the root hair mutant to retain its enriched
529 P-cycling microbiome to booting stage by growing the plants in P-depleted conditions. We
530 speculated that by adding additional P stress, this would initiate a 'cry for help' from the plant
531 that would initiate a response from the bacterial microbiome (Zhang et al., 2025). However,
532 this hypothesis was not supported by the data. We did see an enrichment of *Kitatasatospora*
533 in the root hair mutant rhizosphere at GS45-47 in low-P soil, a plant-associated genus that
534 has been indicated in P cycling (Oliveira et al., 2009), but this was not reflected in the functional
535 profiling. The relative abundances of all bacterial P-cycling genes were equal between the root
536 hair mutant and the wild-type. On the other hand, we saw a fungal response in the root hair
537 mutant under these conditions. Total AMF colonization was equal in the root hair mutant in
538 wild-type during booting under low-P conditions, a well-known response of plants grown in P-
539 depleted conditions (Breuillin et al., 2010; Kumar et al., 2019; Zhou et al., 2022). However,
540 arbuscule formation was higher in the root hair mutant compared to the wild-type and
541 increased compared to growth in P-replete conditions. Arbuscules are the specialized
542 mycorrhizal structures that facilitate mineral nutrient translocation from fungus to plant (Smith
543 & Smith, 2011). This result further supports the dominance of AMF in root hair mutants
544 compared to bacteria.

545 Despite decades of research, successfully manipulating the rhizosphere microbiome for
546 improved crop nutrition remains limited. Our results shed light on how a wheat mutant,
547 defective in root hair elongation, can enrich bacterial and fungal partners for P nutrition. We
548 suggest a temporal component to plant-microbiome interactions that play a role in P nutrition.
549 A practical implication of our findings is that, given genotypic variation in root hair length within
550 elite wheat germplasm (Delhaize et al., 2015), the genotypes with constitutively short root
551 hairs or poor plasticity (Nguyen & Stangoulis, 2019) are likely to enlist microbial mechanisms
552 to ensure P nutrition. Collectively, this work can be used to guide improvements of microbial
553 P uptake mechanisms in wheat. By considering the natural ecology in the rhizosphere of the
554 root hair mutant, we recommend focusing on bacterial interactions only during the early stages
555 of wheat development and otherwise prioritizing the AMF symbiosis throughout wheat growth.

556

Acknowledgements

The authors thank Andrew Riche (Rothamsted Research, Harpenden, UK) for access to the high- and low-P managed soils. This study was funded by the Novo Nordisk Foundation (Grant number: NNF19SA0059360) and the Biotechnology and Biological Sciences Research Council (BBSRC) as part of the Collaborative Training Program for Sustainable Agricultural Innovation (CTP-SAI) (grant BB/W009439/1) in partnership with The Morley Agricultural Foundation (TMAF). We thank Stephen Rawsthorne (TMAF) and Jonathan Atkinson (University of Nottingham, UK) for their inputs into IT's PhD. Further support to CHH was provided by the European Molecular Biology Organization (EMBO) and the Monogram Network.

Competing interests

The authors declare no competing interests that may influence the outcome of this work.

Author Contributions

Courtney Horn Herms: design of the research; performance of the research; data analysis, collection, or interpretation; writing the manuscript. Ian Tsang: data analysis, collection, or interpretation. Frederik Bak: data analysis, collection, or interpretation; writing the manuscript. Klara Gunnarsen: data analysis, performance of the research; collection, or interpretation; writing the manuscript. Magdalena Hasenzagl: data analysis, collection, or interpretation. Amaru Miranda Djurhuus: data analysis, performance of the research; collection, or interpretation; writing the manuscript. Tom Thirkell: data analysis, collection, or interpretation; writing the manuscript. Eric Ober: design of the research; data analysis, collection, or interpretation; writing the manuscript. Fiona Leigh: writing the manuscript. James Cockram: writing the manuscript. Mette Haubjerg Nicolaisen: design of the research; data analysis, collection, or interpretation; writing the manuscript.

Data Availability

16S rRNA amplicon sequence data is publicly available on NCBI under BioProject PRJNA1308004. Raw data is presented in the figures when appropriate. All other raw data is available upon request.

589 ## References

590 An, R., & Moe, L. A. (2016). Regulation of Pyrroloquinoline Quinone-Dependent Glucose
591 Dehydrogenase Activity in the Model Rhizosphere-Dwelling Bacterium Pseudomonas putida KT2440.
592 *Applied and Environmental Microbiology*, *82*(16), 4955–4964. https://doi.org/10.1128/AEM.00813-
593 16

594 Andersen, K. S., Kirkegaard, R. H., Karst, S. M., & Albertsen, M. (2018). ampvis2: An R package to
595 analyse and visualise 16S rRNA amplicon data. *bioRxiv*. https://doi.org/10.1101/299537

596 Bates, T. R., & Lynch, J. P. (1996). Stimulation of root hair elongation in Arabidopsis thaliana by low
597 phosphorus availability. *Plant, Cell & Environment*, *19*(5), 529–538. https://doi.org/10.1111/j.1365-
598 3040.1996.tb00386.x

599 Bodenhausen, N., Deslandes-Hérold, G., Waelchli, J., Held, A., van der Heijden, M. G. A., & Schlaeppi,
600 K. (2021). Relative qPCR to quantify colonization of plant roots by arbuscular mycorrhizal fungi.
601 *Mycorrhiza*, *31*(2), 137–148. https://doi.org/10.1007/s00572-020-01014-1

602 Breuillin, F., Schramm, J., Hajirezaei, M., Ahkami, A., Favre, P., Druege, U., Hause, B., Bucher, M.,
603 Kretzschmar, T., Bossolini, E., Kuhlemeier, C., Martinoia, E., Franken, P., Scholz, U., & Reinhardt, D.
604 (2010). Phosphate systemically inhibits development of arbuscular mycorrhiza in Petunia hybrida
605 and represses genes involved in mycorrhizal functioning. *The Plant Journal*, *64*(6), 1002–1017.
606 https://doi.org/10.1111/j.1365-313X.2010.04385.x

607 Brundrett, M., Bougher, N., Dell, B., Grove, T., & Malajczuk, N. (1996). *Working with Mycorrhizas in*
608 *Forestry and Agriculture*. https://doi.org/10.13140/2.1.4880.5444

609 Buddrus-Schiemann, K., Schmid, M., Schreiner, K., Welzl, G., & Hartmann, A. (2010). Root
610 Colonization by Pseudomonas sp. DSMZ 13134 and Impact on the Indigenous Rhizosphere Bacterial
611 Community of Barley. *Microbial Ecology*, *60*(2), 381–393. https://doi.org/10.1007/s00248-010-9720-
612 8

613 Callahan, B. J., McMurdie, P. J., Rosen, M. J., Han, A. W., Johnson, A. J. A., & Holmes, S. P. (2016).
614 DADA2: High-resolution sample inference from Illumina amplicon data. *Nature Methods*, *13*(7), 581–
615 583. https://doi.org/10.1038/nmeth.3869

616 De Coster, W., D'Hert, S., Schultz, D. T., Cruts, M., & Van Broeckhoven, C. (2018). NanoPack:
617 Visualizing and processing long-read sequencing data. *Bioinformatics*, *34*(15), 2666–2669.
618 https://doi.org/10.1093/bioinformatics/bty149

619 Delhaize, E., Rathjen, T. M., & Cavanagh, C. R. (2015). The genetics of rhizosheath size in a
620 multiparent mapping population of wheat. *Journal of Experimental Botany*, *66*(15), 4527–4536.
621 https://doi.org/10.1093/jxb/erv223

622 Fox, J., & Weisberg, S. (2019). *An R Companion to Applied Regression* (Third). Sage.
623 https://www.john-fox.ca/Companion/

624 Gahoonia, T. S., Nielsen, N. E., Joshi, P. A., & Jahoor, A. (2001). A root hairless barley mutant for
625 elucidating genetic of root hairs and phosphorus uptake. *Plant and Soil*, *235*(2), 211–219.
626 https://doi.org/10.1023/A:1011993322286

627 Guan, Y., Bak, F., Hennessy, R. C., Horn Herms, C., Elberg, C. L., Dresbøll, D. B., Winding, A., Sapkota,
628 R., & Nicolaisen, M. H. (2024). The potential of Pseudomonas fluorescens SBW25 to produce viscosin

enhances wheat root colonization and shapes root-associated microbial communities in a plant genotype-dependent manner in soil systems. *mSphere*, *9*(7), e00294-24. https://doi.org/10.1128/msphere.00294-24

Haling, R. E., Brown, L. K., Bengough, A. G., Young, I. M., Hallett, P. D., White, P. J., & George, T. S. (2013). Root hairs improve root penetration, root–soil contact, and phosphorus acquisition in soils of different strength. *Journal of Experimental Botany*, *64*(12), 3711–3721. https://doi.org/10.1093/jxb/ert200

Hao, X., Zhu, Y.-G., Nybroe, O., & Nicolaisen, M. H. (2020). The Composition and Phosphorus Cycling Potential of Bacterial Communities Associated With Hyphae of Penicillium in Soil Are Strongly Affected by Soil Origin. *Frontiers in Microbiology*, *10*. https://doi.org/10.3389/fmicb.2019.02951

Helgason, T., Daniell, T. J., Husband, R., Fitter, A. H., & Young, J. P. W. (1998). Ploughing up the wood-wide web? *Nature*, *394*(6692), 431–431. https://doi.org/10.1038/28764

Herms, C. H., Hennessy, R. C., Bak, F., Guan, Y., Browne, P. D., Nielsen, T. K., Hansen, L. H., Dresbøll, D. B., & Nicolaisen, M. H. (2025). *Pseudomonas* taxonomic and functional microdiversity in the wheat rhizosphere is cultivar-dependent and links to disease resistance profile and root diameter. *Applied Soil Ecology*, *211*, 106116. https://doi.org/10.1016/j.apsoil.2025.106116

Hewins, C. R., Carrino-Kyker, S. R., & Burke, D. J. (2015). Seasonal variation in mycorrhizal fungi colonizing roots of Allium tricoccum (wild leek) in a mature mixed hardwood forest. *Mycorrhiza*, *25*(6), 469–483. https://doi.org/10.1007/s00572-015-0628-5

Jakobsen, I., Chen, B., Munkvold, L., Lundsgaard, T., & Zhu, Y.-G. (2005). Contrasting phosphate acquisition of mycorrhizal fungi with that of root hairs using the root hairless barley mutant. *Plant, Cell & Environment*, *28*(7), 928–938. https://doi.org/10.1111/j.1365-3040.2005.01345.x

Jansa, J., Erb, A., Oberholzer, H.-R., Šmilauer, P., & Egli, S. (2014). Soil and geography are more important determinants of indigenous arbuscular mycorrhizal communities than management practices in Swiss agricultural soils. *Molecular Ecology*, *23*(8), 2118–2135. https://doi.org/10.1111/mec.12706

Jaspers, E., & Overmann, J. (2004). Ecological Significance of Microdiversity: Identical 16S rRNA Gene Sequences Can Be Found in Bacteria with Highly Divergent Genomes and Ecophysiologies. *Applied and Environmental Microbiology*, *70*(8), 4831–4839. https://doi.org/10.1128/AEM.70.8.4831-4839.2004

Jones, C., Olson-Rutz, K., & Dinkins, C. (2024, March). *Nutrient Uptake Timing by Crops to Assist with Fertilizing Decisions*. Montana State University Extension.

Krasileva, K. V., Vasquez-Gross, H. A., Howell, T., Bailey, P., Paraiso, F., Clissold, L., Simmonds, J., Ramirez-Gonzalez, R. H., Wang, X., Borrill, P., Fosker, C., Ayling, S., Phillips, A. L., Uauy, C., & Dubcovsky, J. (2017). Uncovering hidden variation in polyploid wheat. *Proceedings of the National Academy of Sciences*, *114*(6), E913–E921. https://doi.org/10.1073/pnas.1619268114

Kumar, A., Rithesh, L., Kumar, V., Raghuvanshi, N., Chaudhary, K., Abhineet, & Pandey, A. K. (2023). Stenotrophomonas in diversified cropping systems: Friend or foe? *Frontiers in Microbiology*, *14*. https://doi.org/10.3389/fmicb.2023.1214680

Kumar, A., Shahbaz, M., Koirala, M., Blagodatskaya, E., Seidel, S. J., Kuzyakov, Y., & Pausch, J. (2019). Root trait plasticity and plant nutrient acquisition in phosphorus limited soil. *Journal of Plant Nutrition and Soil Science*, *182*(6), 945–952. https://doi.org/10.1002/jpln.201900322

Ma, X., Li, X., & Ludewig, U. (2020). Arbuscular mycorrhizal colonization outcompetes root hairs in maize under low phosphorus availability. *Annals of Botany*, *127*(1), 155. https://doi.org/10.1093/aob/mcaa159

Marrassini, V., Ercoli, L., Piazza, G., & Pellegrino, E. (2024). Plant genotype and inoculation with indigenous arbuscular mycorrhizal (AM) fungi modulate wheat productivity and quality of processed products through changes in the frequency of root AM fungal taxa. *Field Crops Research*, *315*, 109456. https://doi.org/10.1016/j.fcr.2024.109456

Martin, B. D., Witten, D., & Willis, A. D. (2020). Modeling microbial abundances and dysbiosis with beta-binomial regression. *The Annals of Applied Statistics*, *14*(1), 94–115. https://doi.org/10.1214/19-AOAS1283

Martin, M. (2011). Cutadapt removes adapter sequences from high-throughput sequencing reads. *EMBnet.Journal*, *17*(1), Article 1. https://doi.org/10.14806/ej.17.1.200

Matthus, E., Zwetsloot, M., Delory, B. M., Hennecke, J., Andraczek, K., Henning, T., Mommer, L., Weigelt, A., & Bergmann, J. (2025). Revisiting the root economics space—Its applications, extensions and nuances advance our understanding of fine-root functioning. *Plant and Soil*, *514*(1), 1–27. https://doi.org/10.1007/s11104-025-07379-6

McMurdie, P. J., & Holmes, S. (2013). phyloseq: An R Package for Reproducible Interactive Analysis and Graphics of Microbiome Census Data. *PLOS ONE*, *8*(4), e61217. https://doi.org/10.1371/journal.pone.0061217

Menezes-Blackburn, D., Giles, C., Darch, T., George, T. S., Blackwell, M., Stutter, M., Shand, C., Lumsdon, D., Cooper, P., Wendler, R., Brown, L., Almeida, D. S., Wearing, C., Zhang, H., & Haygarth, P. M. (2018). Opportunities for mobilizing recalcitrant phosphorus from agricultural soils: A review. *Plant and Soil*, *427*(1), 5–16. https://doi.org/10.1007/s11104-017-3362-2

Mousa, W. K., Shearer, C., Limay-Rios, V., Ettinger, C. L., Eisen, J. A., & Raizada, M. N. (2016). Root-hair endophyte stacking in finger millet creates a physicochemical barrier to trap the fungal pathogen Fusarium graminearum. *Nature Microbiology*, *1*(12), 1–12. https://doi.org/10.1038/nmicrobiol.2016.167

Murphy, J., & Riley, J. P. (1962). A modified single solution method for the determination of phosphate in natural waters. *Analytica Chimica Acta*, *27*, 31–36. https://doi.org/10.1016/S0003-2670(00)88444-5

Nguyen, V. L., & Stangoulis, J. (2019). Variation in root system architecture and morphology of two wheat genotypes is a predictor of their tolerance to phosphorus deficiency. *Acta Physiologiae Plantarum*, *41*(7), 109. https://doi.org/10.1007/s11738-019-2891-0

Nunes, I., Hansen, V., Bak, F., Bonnichsen, L., Su, J., Hao, X., Raymond, N. S., Nicolaisen, M. H., Jensen, L. S., & Nybroe, O. (2022). Succession of the wheat seed-associated microbiome as affected by soil fertility level and introduction of Penicillium and Bacillus inoculants in the field. *FEMS Microbiology Ecology*, *98*(3), fiac028. https://doi.org/10.1093/femsec/fiac028

Oliveira, C. A., Alves, V. M. C., Marriel, I. E., Gomes, E. A., Scotti, M. R., Carneiro, N. P., Guimarães, C. T., Schaffert, R. E., & Sá, N. M. H. (2009). Phosphate solubilizing microorganisms isolated from rhizosphere of maize cultivated in an oxisol of the Brazilian Cerrado Biome. *Soil Biology and Biochemistry*, *41*(9), 1782–1787. https://doi.org/10.1016/j.soilbio.2008.01.012

Phillips, J. M., & Hayman, D. S. (1970). Improved procedures for clearing roots and staining parasitic and vesicular-arbuscular mycorrhizal fungi for rapid assessment of infection. *Transactions of the British Mycological Society*, *55*(1), 158-IN18. https://doi.org/10.1016/S0007-1536(70)80110-3

Qi, P.-F., Johnston, A., Balcerzak, M., Rocheleau, H., Harris, L. J., Long, X.-Y., Wei, Y.-M., Zheng, Y.-L., & Ouellet, T. (2012). Effect of salicylic acid on *Fusarium graminearum*, the major causal agent of fusarium head blight in wheat. *Fungal Biology*, *116*(3), 413–426. https://doi.org/10.1016/j.funbio.2012.01.001

Quast, C., Pruesse, E., Yilmaz, P., Gerken, J., Schweer, T., Yarza, P., Peplies, J., & Glöckner, F. O. (2013). The SILVA ribosomal RNA gene database project: Improved data processing and web-based tools. *Nucleic Acids Research*, *41*(D1), D590–D596. https://doi.org/10.1093/nar/gks1219

Quattrone, A., Lopez-Guerrero, M., Yadav, P., Meier, M. A., Russo, S. E., & Weber, K. A. (2024). Interactions between root hairs and the soil microbial community affect the growth of maize seedlings. *Plant, Cell & Environment*, *47*(2), 611–628. https://doi.org/10.1111/pce.14755

R Core Team. (2023). *R: A Language and Environment for Statistical Computing*. R Foundation for Statistical Computing. https://www.R-project.org/

Raymond, N. S., Gómez-Muñoz, B., van der Bom, F. J. T., Nybroe, O., Jensen, L. S., Müller-Stöver, D. S., Oberson, A., & Richardson, A. E. (2021). Phosphate-solubilising microorganisms for improved crop productivity: A critical assessment. *New Phytologist*, *229*(3), 1268–1277. https://doi.org/10.1111/nph.16924

Rengel, Z., Cakmak, I., & White, P. J. (2022). *Marschner's Mineral Nutrition of Plants*. Academic Press.

Richardson, A. E., Lynch, J. P., Ryan, P. R., Delhaize, E., Smith, F. A., Smith, S. E., Harvey, P. R., Ryan, M. H., Veneklaas, E. J., Lambers, H., Oberson, A., Culvenor, R. A., & Simpson, R. J. (2011). Plant and microbial strategies to improve the phosphorus efficiency of agriculture. *Plant and Soil*, *349*(1), 121–156. https://doi.org/10.1007/s11104-011-0950-4

Robertson-Albertyn, S., Alegria Terrazas, R., Balbirnie, K., Blank, M., Janiak, A., Szarejko, I., Chmielewska, B., Karcz, J., Morris, J., Hedley, P. E., George, T. S., & Bulgarelli, D. (2017). Root Hair Mutations Displace the Barley Rhizosphere Microbiota. *Frontiers in Plant Science*, *8*, 1–15. https://doi.org/10.3389/fpls.2017.01094

Ruijter, J. M., Ramakers, C., Hoogaars, W. M. H., Karlen, Y., Bakker, O., van den Hoff, M. J. B., & Moorman, A. F. M. (2009). Amplification efficiency: Linking baseline and bias in the analysis of quantitative PCR data. *Nucleic Acids Research*, *37*(6), e45. https://doi.org/10.1093/nar/gkp045

Saunders, W. M. H., & Williams, E. G. (1955). Observations on the Determination of Total Organic Phosphorus in Soils. *Journal of Soil Science*, *6*(2), 254–267. https://doi.org/10.1111/j.1365-2389.1955.tb00849.x

Schloss, P. D. (2024). Rarefaction is currently the best approach to control for uneven sequencing effort in amplicon sequence analyses. *mSphere*, *9*(2), e00354-23. https://doi.org/10.1128/msphere.00354-23

Simonin, M., Briand, M., Chesneau, G., Rochefort, A., Marais, C., Sarniguet, A., & Barret, M. (2022). Seed microbiota revealed by a large-scale meta-analysis including 50 plant species. *New Phytologist*, *234*(4), 1448–1463. https://doi.org/10.1111/nph.18037

Simpson, R. J., Oberson, A., Culvenor, R. A., Ryan, M. H., Veneklaas, E. J., Lambers, H., Lynch, J. P., Ryan, P. R., Delhaize, E., Smith, F. A., Smith, S. E., Harvey, P. R., & Richardson, A. E. (2011). Strategies and agronomic interventions to improve the phosphorus-use efficiency of farming systems. *Plant and Soil*, *349*(1), 89–120. https://doi.org/10.1007/s11104-011-0880-1

Smith, S. E., & Smith, F. A. (2011). Roles of arbuscular mycorrhizas in plant nutrition and growth: New paradigms from cellular to ecosystem scales. *Annual Review of Plant Biology*, *62*, 227–250. https://doi.org/10.1146/annurev-arplant-042110-103846

Suzuki, N., Taketa, S., & Ichii, M. (2003). Morphological and physiological characteristics of a root-hairless mutant in rice (Oryza sativa L.). *Plant and Soil*, *255*(1), 9–17. https://doi.org/10.1023/A:1026180318923

Tang, J., Wu, D., Li, X., Wang, L., Xu, L., Zhang, Y., Xu, F., Liu, H., Xie, Q., Dai, S., Coleman-Derr, D., Zhu, S., & Yu, F. (2022). Plant immunity suppression via PHR1-RALF-FERONIA shapes the root microbiome to alleviate phosphate starvation. *The EMBO Journal*, *41*(6), EMBJ2021109102. https://doi.org/10.15252/embj.2021109102

Thijs, S., Op De Beeck, M., Beckers, B., Truyens, S., Stevens, V., Van Hamme, J. D., Weyens, N., & Vangronsveld, J. (2017). Comparative Evaluation of Four Bacteria-Specific Primer Pairs for 16S rRNA Gene Surveys. *Frontiers in Microbiology*, *8*. https://doi.org/10.3389/fmicb.2017.00494

Thirkell, T. J., Pastok, D., & Field, K. J. (2020). Carbon for nutrient exchange between arbuscular mycorrhizal fungi and wheat varies according to cultivar and changes in atmospheric carbon dioxide concentration. *Global Change Biology*, *26*(3), 1725–1738. https://doi.org/10.1111/gcb.14851

Tsang, I., Thomelin, P., Ober, E. S., Rawsthorne, S., Atkinson, J. A., Wells, D. M., Percival-Alwyn, L., Leigh, F. J., & Cockram, J. (2024). A novel root hair mutant, srh1, affects root hair elongation and reactive oxygen species levels in wheat. *Frontiers in Plant Science*, *15*. https://doi.org/10.3389/fpls.2024.1490502

Ulén, B., Bechmann, M., Fölster, J., Jarvie, H. P., & Tunney, H. (2007). Agriculture as a phosphorus source for eutrophication in the north-west European countries, Norway, Sweden, United Kingdom and Ireland: A review. *Soil Use and Management*, *23*(s1), 5–15. https://doi.org/10.1111/j.1475-2743.2007.00115.x

Van Kauwenbergh, S. (2010). *World Phosphate Rock Reserves and Resources*. IFDC Publications. https://pdf.usaid.gov/pdf_docs/Pnadw835.PDF

Wang, L., Zhou, J., George, T. S., & Feng, G. (2025). Trade-offs between arbuscular mycorrhizal symbiosis and root hairs in phosphorus source utilization are determined by functional divergence of the rhizosphere bacterial microbiome in barley. *Soil Biology and Biochemistry*, *209*, 109887. https://doi.org/10.1016/j.soilbio.2025.109887

Werner, G. D. A., & Kiers, E. T. (2015). Order of arrival structures arbuscular mycorrhizal colonization of plants. *New Phytologist*, *205*(4), 1515–1524. https://doi.org/10.1111/nph.13092

Wickham, H. (2016). *ggplot2: Elegant Graphics for Data Analysis*. Springer-Verlag New York. https://ggplot2.tidyverse.org

Xiong, C., Singh, B. K., He, J.-Z., Han, Y.-L., Li, P.-P., Wan, L.-H., Meng, G.-Z., Liu, S.-Y., Wang, J.-T., Wu, C.-F., Ge, A.-H., & Zhang, L.-M. (2021). Plant developmental stage drives the differentiation in ecological role of the maize microbiome. *Microbiome*, *9*(1), 171. https://doi.org/10.1186/s40168-021-01118-6

Yi, H., Hu, S., Zhang, Y., Wang, X., Xia, Z., Lei, Y., & Duan, M. (2023). Proper Delay of Phosphorus Application Promotes Wheat Growth and Nutrient Uptake under Low Phosphorus Condition. *Agriculture*, *13*(4), Article 4. https://doi.org/10.3390/agriculture13040884

Zadoks, J. C., Chang, T. T., & Konzak, C. F. (1974). A decimal code for the growth stages of cereals. *Weed Research*, *14*(6), 415–421. https://doi.org/10.1111/j.1365-3180.1974.tb01084.x

Zhang, L., Deng, X., Xiao, J., Zhao, W., Zou, P., Liao, R., Xie, K., & Liao, H. (2025). Root metabolites regulated by FERONIA promote phosphorus-solubilizing rhizobacteria enrichment induced by *Arabidopsis thaliana* coping with phosphorus deficiency. *Microbiological Research*, *292*, 128030. https://doi.org/10.1016/j.micres.2024.128030

Zhou, J., Zhang, L., Feng, G., & George, T. S. (2022). Arbuscular mycorrhizal fungi have a greater role than root hairs of maize for priming the rhizosphere microbial community and enhancing rhizosphere organic P mineralization. *Soil Biology and Biochemistry*, *171*, 108713. https://doi.org/10.1016/j.soilbio.2022.108713

Zhu, R., Chen, C., Chen, M., Miroslav, V., Dao, J., Xing, Y., Kong, D., Chen, B., & Wang, Z. (2025). How Arbuscular Mycorrhizal Fungi Shape Plant Root Morphology: A Global Meta-Analysis. *Plant, Cell & Environment*. https://doi.org/10.1111/pce.70082